

Misfit Strain Induced Tweed-Twin Transformation on Composition Modulation $Zn_{1-x}Mg_xS_ySe_{1-y}$ Layers and the Quality Control of the ZnSe Buffer/GaAs Interface

L.H. KUO and L. SALAMANCA-RIBA

Department of Materials and Nuclear Engineering, University of Maryland, College Park, MD 20742-2115

B.J. WU and J.M. DE PUYDT

3M Company, St. Paul, MN 55144-1000

[100] composition modulation as well as [101] and $[\bar{1}01]$ tweed strain contrast were observed in 0.72 μm thick $Zn_{1-x}Mg_xS_ySe_{1-y}$ epitaxial films grown on ZnSe buffer layers. The lattice distortion induced tweed strain contrast disappears in relaxed $Zn_{1-x}Mg_xS_ySe_{1-y}$ layers of thicknesses above $\sim 0.8\text{--}1\ \mu\text{m}$ even though the [100] composition modulation remains. Instead, the formation of microtwins takes place to relieve the strain in the distorted lattice of the quaternary films. The $Zn_{1-x}Mg_xS_ySe_{1-y}$ layers were obtained by growing a ZnSe buffer layer on As-stabilized GaAs substrates with Zn treatment of the substrate prior to the growth of the film. The samples with film thickness of $\sim 0.72\ \mu\text{m}$ were of very high quality with a defect density of less than $5 \times 10^4/\text{cm}^2$. Some samples showed rough ZnSe/GaAs interfaces and a high density of Frank partial dislocations originating at the ZnSe/GaAs interface. The interface roughness is believed to result from an As-rich GaAs surface after the oxide desorption.

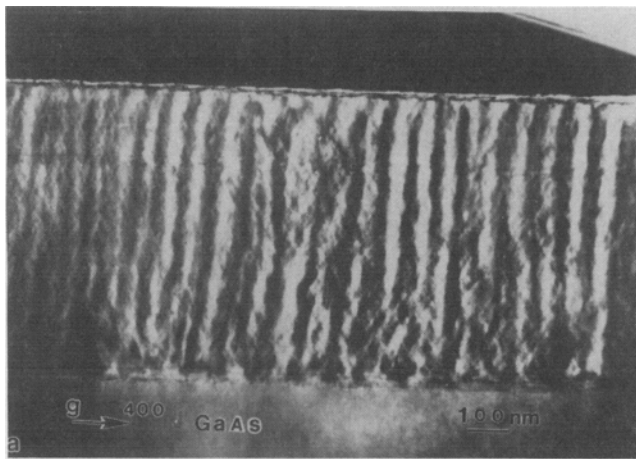
Key words: Composition modulation, misfit accommodation, $Zn_{1-x}Mg_xS_ySe_{1-y}$ films, twinning

INTRODUCTION

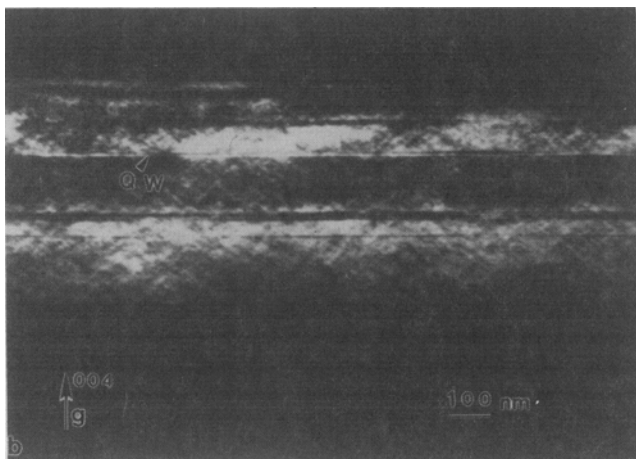
The first green II-VI injection lasers have been fabricated by Haase et al.¹ and later by Jeon et al.,² using $ZnS_{0.06}Se_{0.94}$ as cladding layers with a ZnSe waveguiding region. Recently, a new material, $Zn_{1-x}Mg_xS_ySe_{1-y}$ with high magnesium and sulfur concentrations ($x, y \geq 0.15$), was proposed and studied for the fabrication of blue-light emitting devices.³ In this study, a double heterostructure containing a thin $ZnS_{0.06}Se_{0.94}$ active layer and a quaternary $Zn_{1-x}Mg_xS_ySe_{1-y}$ cladding layer were used. Also, for blue-green lasing, the first pseudomorphic separate-confinement diode with $Zn_{0.9}Mg_{0.1}S_{0.1}Se_{0.9}$ cladding and $ZnS_{0.06}Se_{0.94}$ guiding layers in the pulsed mode has been demonstrated at room temperature.⁴ Due to the differences in band gap energy between the guiding and $Zn_{1-x}Mg_xS_ySe_{1-y}$ cladding layers with different

magnesium and sulfide concentrations, blue or blue-green light emitting devices are possible.⁴⁻⁷ For materials consideration, since the tetrahedral covalent radius of magnesium is larger than that of zinc and the tetragonal covalent radius of sulfur is smaller than that of selenium,⁸ the lattice constant of $Zn_{1-x}Mg_xS_ySe_{1-y}$ films can be adjusted to obtain pseudomorphic cladding layers with in-plane lattice constant equal to that of GaAs. Besides, the band gap energy can be increased by increasing the sulfur concentration and the material can remain pseudomorphic to the GaAs substrate.³ Thus, on the growth of the $Zn_xMg_{1-x}S_ySe_{1-y}$ film, the band gap energy can be tuned to obtain blue-green or blue lasing and the lattice constant can be adjusted to match the lattice constant of the GaAs substrate.

The growth of lattice matched quaternaries requires exact control and high stability of the fluxes. We investigated the microstructure of quaternary $Zn_{1-x}Mg_xS_ySe_{1-y}$ layers of different film thicknesses



a



b

Fig. 1. Transmission electron microscopy (010) cross section (a) (400) and (b) (004) dark field images of a $\sim 200\text{\AA}$ ZnSe cap layer/ $\sim 0.18\ \mu\text{m}$ $\text{Zn}_{0.726}\text{Mg}_{0.274}\text{S}_{0.265}\text{Se}_{0.735}$ / $\sim 88\text{\AA}$ ZnSe QW/ $\sim 0.54\ \mu\text{m}$ $\text{Zn}_{0.726}\text{Mg}_{0.274}\text{S}_{0.265}\text{Se}_{0.735}$ / $\sim 266\text{\AA}$ ZnSe buffer/GaAs sample. Both composition modulation and tweed contrast are observed in (a), but only tweed contrast is observed in (b).

but with approximately the same composition. We also studied the quality of the ZnSe buffer/GaAs interface. We have previously reported⁹ the observation of composition modulation in pseudomorphic $\text{Zn}_{1-x}\text{Mg}_x\text{S}_y\text{Se}_{1-y}$ films.

In the present work, we compare the composition modulation in strained and relaxed $\text{Zn}_{1-x}\text{Mg}_x\text{S}_y\text{Se}_{1-y}$ layers and discuss the mechanism for strain relaxation. Both pseudomorphic and relaxed $\text{Zn}_{1-x}\text{Mg}_x\text{S}_y\text{Se}_{1-y}$ layers with total film thicknesses of ~ 0.72 to $2.1\ \mu\text{m}$ were grown on GaAs substrates with ZnSe buffer layers. The ZnSe buffer layer was grown between the quaternary $\text{Zn}_x\text{Mg}_{1-x}\text{S}_y\text{Se}_{1-y}$ film and the GaAs substrate to decrease the density of faulted defects generated on the II-VI/GaAs interface. The quaternary $\text{Zn}_{1-x}\text{Mg}_x\text{S}_y\text{Se}_{1-y}$ films contained relatively high magnesium and sulfur concentrations ($\sim 0.24 \leq x \leq 0.28$ and $\sim 0.26 \leq y \leq 0.33$) to obtain a high band gap energy of $\sim 3.1\ \text{eV}$. For films with thicknesses below $0.8\text{--}1\ \mu\text{m}$, the quaternary films were pseudomorphic to the GaAs substrate giving rise to a tweed structure originating

at the $\text{Zn}_{1-x}\text{Mg}_x\text{S}_y\text{Se}_{1-y}$ /ZnSe interface. However, for relaxed quaternary layers with film thickness of $\sim 2.1\ \mu\text{m}$, the lattice strain relaxed by the formation of microtwins mostly originating at the $\text{Zn}_{1-x}\text{Mg}_x\text{S}_y\text{Se}_{1-y}$ /ZnSe interface. In both cases, however, chemical composition modulation was found in the quaternary films.

The formation of defects in epilayers also affects the performance of semiconductor devices. Defects could either act as pinning centers for electronic carriers or as sources for the formation of degradation defects.¹⁰ From our studies, Frank partial dislocations were observed originating at the ZnSe buffer/GaAs interface. No Shockley partial dislocations were observed for these ZnSe layers with two dimensional (2D) growth mode on GaAs substrates. The density of faulted defects is greatly dependent on the treatment and stoichiometry of the GaAs surface.

EXPERIMENTAL

The $\text{Zn}_{1-x}\text{Mg}_x\text{S}_y\text{Se}_{1-y}$ epilayers studied in this work were grown on ZnSe buffer layers on (001) GaAs substrates by molecular beam epitaxy (MBE). The films were grown at 280°C under ZnS, Mg, and Se atmospheres at a growth rate of $0.7\ \mu\text{m}/\text{h}$.¹¹ The GaAs substrates were desorbed inside a separate chamber with As over pressure. The As-terminated substrates were then transferred to the growth chamber and heated to the growth temperature. In this chamber a (2×1) reconstructed surface was obtained. Then the substrates were exposed to Zn for ~ 2 min before the growth of the ZnSe buffer layers was initiated. After the Zn treatment, the growth surface became smoother as evidenced by a more streaky and sharp (2×1) reflection high energy electron diffraction (RHEED) pattern.

The films were grown in the two-dimensional (2D) mode as observed by RHEED studies. The total film thicknesses were between 0.72 to $2.1\ \mu\text{m}$, as measured by transmission electron microscopy (TEM). A JEOL 840 scanning electron microscope (SEM) was used to identify the density of the defects using cathodoluminescence (CL). A Bede 150 double crystal rocking curve system was used to determine the vertical lattice constant of the $\text{Zn}_{1-x}\text{Mg}_x\text{S}_y\text{Se}_{1-y}$ film and evaluate the films' quality. The band gap energy was determined by room temperature photoreflectance, and the average composition of the films was determined by the vertical lattice constant and the bandgap energy. For TEM studies, (100), (010), (110), and $(\bar{1}10)$ cross-section specimens were prepared by mechanically thinning the samples using a tripod polisher followed by argon ion-milling at liquid nitrogen temperature. The energy of the Ar^+ ions was 2 to 3 KeV to minimize sample preparation damage. In addition, (001) plan-view specimens were prepared by etching the back side of the substrate using a 4:1 ($\text{H}_2\text{O}_2:\text{NH}_4\text{OH}$) solution. A JEOL 2000FX-II and a JEOL 200 CX TEMs with side entry goniometers operated at 200 KV were used to study the structure of the quaternary films.

RESULTS AND DISCUSSION

Composition Modulation and Tweed Structures in the Pseudomorphic $Zn_{1-x}Mg_xS_ySe_{1-y}$ Films

Figure 1a is a TEM (400) dark field image from a (010) cross-sectional $Zn_{1-x}Mg_xS_ySe_{1-y}$ /ZnSe quantum well (QW)/ $Zn_{1-x}Mg_xS_ySe_{1-y}$ /ZnSe buffer/GaAs heterostructure. The thickness of the ZnSe QW is $\sim 88\text{\AA}$ and is located at a distance of $\sim 0.2\ \mu\text{m}$ from the film surface. The thickness of the ZnSe buffer layer is $\sim 266\text{\AA}$. The total thickness of the film is $\sim 0.72\ \mu\text{m}$. A contrast modulation is observed along the [100] direction (perpendicular to the growth direction) in the $Zn_{1-x}Mg_xS_ySe_{1-y}$ film with a period of ~ 50 to $70\ \text{nm}$. From energy dispersive x-ray spectroscopy (EDS) composition measurements obtained from the dark and bright bands in Fig. 1a, we observed a variation in the S and Mg concentrations indicating that the contrast corresponds to a composition modulation. In addition to the composition modulation contrast, tweed-like strain contrast is also observed in Fig. 1a. The tweed-like contrast is along the [101] and $[\bar{1}01]$ directions, i.e., inclined $\pm 45^\circ$ with respect to the growth surface.

No misfit or threading dislocations were observed in any of the TEM cross-sectional and plan-view images from this sample. Also, the full width at half maximum (FWHM) is of ~ 33 arc s as measured from x-ray rocking curves. These results indicate that the quaternary film is indeed pseudomorphic to the GaAs substrate with good material quality. The projected images of the ZnSe QW and the ZnSe buffer layer overlap with the modulated $Zn_{1-x}Mg_xS_ySe_{1-y}$ image in Fig. 1a because the sample was tilted about the [100] axis to obtain the image. Also, from the TEM cross-sectional images, we observed that the ZnSe QW remains pseudomorphic to the quaternary film with the same in plane lattice constant. Furthermore, from TEM $(\bar{1}10)$, (110), (100), and (010) diffraction patterns, very faint streaks along the [001] growth direction were observed. This indicates that the lattice in the regions of different composition is tetragonally distorted with a varied perpendicular lattice constant (a_\perp) in order to remain pseudomorphic with the GaAs substrate.

Figure 1b is a TEM (004) dark field image from a (010) cross-section of the same sample shown in Fig. 1a. In contrast to Fig. 1a, Fig. 1b shows no contrast for the composition modulation and only tweed-like strain contrast distributed throughout the modulated $Zn_{1-x}Mg_xS_ySe_{1-y}$ film (except in the area of the ZnSe QW and the buffer layer) is observed. The invisibility of the composition modulation contrast in the [004] two-beam condition indicates that the decomposition of the $Zn_{1-x}Mg_xS_ySe_{1-y}$ film is in the direction normal to the growth direction only. (100) and (110) high resolution TEM (HRTEM) images from this sample show that the composition modulation of the $Zn_{1-x}Mg_xS_ySe_{1-y}$ starts at the ZnSe buffer layer/

$Zn_{1-x}Mg_xS_ySe_{1-y}$ interface. No satellite spots associated with the composition modulation were observed due to the resolution of the TEM diffraction spots for these large wavelengths (~ 50 to $70\ \text{nm}$) of composition-modulation.

Origin of Tweed Structures

Another strain contrast in the pseudomorphic $Zn_{1-x}Mg_xS_ySe_{1-y}$ films is the tweed-like contrast observed in Fig. 1 of the TEM cross-sectional images. Figure 1b shows that the tweed-like strain contrast which is also associated with the composition modulation⁹ starts at the ZnSe buffer/ $Zn_{1-x}Mg_xS_ySe_{1-y}$ interface. From TEM $(\bar{1}10)$, (110), (100), and (010) diffraction patterns, very faint streaky diffraction spots along the [001] growth direction were observed. This indicates that the lattice in the regions of different composition is tetragonally distorted with a varied perpendicular lattice constant (a_\perp) in order to remain pseudomorphic with the GaAs substrate. Thus, the film/substrate interface is coherent but there is strain along the growth direction. This indicated that the composition modulation produces different tetragonality in areas of different composition giving rise to a waviness of the lattice spacing a_\perp along the growth direction. The waviness of the planes produces strain modulation which is observed as tweed contrast. This kind of tweed strain contrast has been observed in $In_{1-x}Ga_xAs_yP_{1-y}$ epitaxial films.¹² However, in relaxed III-V and IV-VI epitaxial films,^{13,14} no such tweed strain contrast was observed even though composition modulation was found. This is because no local variation in the tetragonality of the films was expected in the relaxed modulated structures.

The origin of the tweed contrast in Ni-Al alloys, for

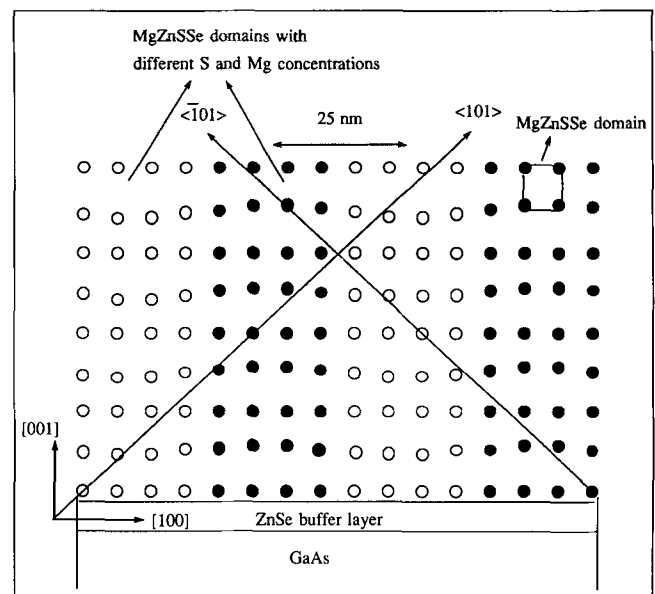


Fig. 2. Schematic diagram of the $Zn_{1-x}Mg_xS_ySe_{1-y}$ /ZnSe buffer/GaAs heterostructure with composition modulation and strain modulation starting from the $Zn_{1-x}Mg_xS_ySe_{1-y}$ /ZnSe interface. The $Zn_{1-x}Mg_xS_ySe_{1-y}$ domains remain pseudomorphic to the GaAs substrate with localized variations of the tetragonal distortion of the lattice along the growth direction.

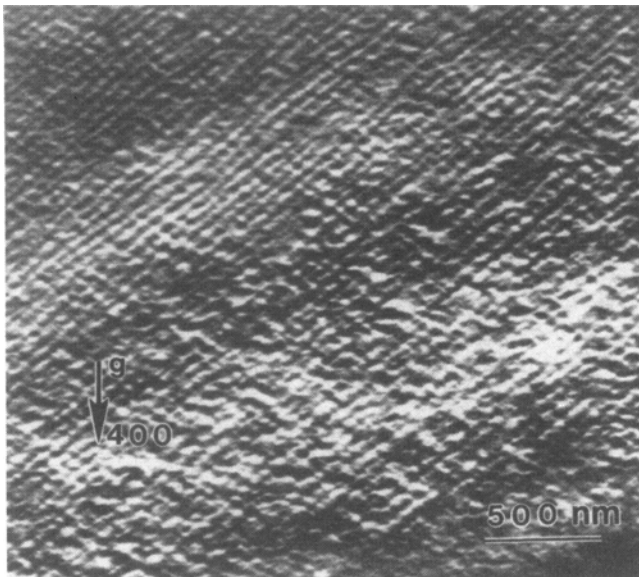


Fig. 3. (400) dark field plan-view image of a $\text{Zn}_{1-x}\text{Mg}_x\text{S}_y\text{Se}_{1-y}$ film. Strain modulation contrast induced by surface buckling is observed along the [110] direction and the striated composition modulation contrast is observed along the [100] direction.

example, has been demonstrated by Roberston and Wayman¹⁵ to arise from a localized variation in the tetragonal distortion of the lattice by the static displacements of atoms. In $\text{Zn}_{1-x}\text{Mg}_x\text{S}_y\text{Se}_{1-y}$ films, Mg has a larger tetrahedral covalent radius than Zn, and the tetrahedral covalent radius of S is smaller than that of Se.⁸ Thus, the difference in tetrahedral covalent radii produces clustering of like species which in turn introduce local dilations and contractions of the lattice, as has been discussed in Ni-Al alloys.¹⁵ The tweed structure may or may not coexist with the modulated structure. However, the localized variation in distortion of the lattice by the static displacements of atoms seems to have a direct correlation with the tweed strain contrast. No such local dilations and contractions of the lattice are expected in the binary ZnSe compound. Thus, it is not surprising that no tweed contrast was observed in the ZnSe QW or buffer layers. Besides, in pseudomorphic $\text{Zn}_{0.9}\text{Mg}_{0.1}\text{S}_{0.1}\text{Se}_{0.9}$ films with low Mg concentration,⁴ no composition modulation or tweed structures were observed. Thus, there seems to be a minimum in the Mg and S concentration necessary to produce enough localized tetragonal perturbations of the lattice. A possible schematic diagram of the distortions in $\text{Zn}_{1-x}\text{Mg}_x\text{S}_y\text{Se}_{1-y}$ films is presented in Fig. 2. This figure shows domains with a specific out of plane interplanar spacing and not individual unit cells. The $\text{Zn}_{1-x}\text{Mg}_x\text{S}_y\text{Se}_{1-y}$ film remains pseudomorphic to the ZnSe buffer layer and GaAs substrate and thus has the same parallel lattice constant, a_{\parallel} . The modulation in the composition is along the [100] direction with a modulation period of ~50 nm. Along the [001] growth direction, the quaternary domains maintain coherency with varying tetragonal distortion for the domains with different composition. In this fashion, the lattice in the $\text{Zn}_{1-x}\text{Mg}_x\text{S}_y\text{Se}_{1-y}$ film is distorted along the [101] and

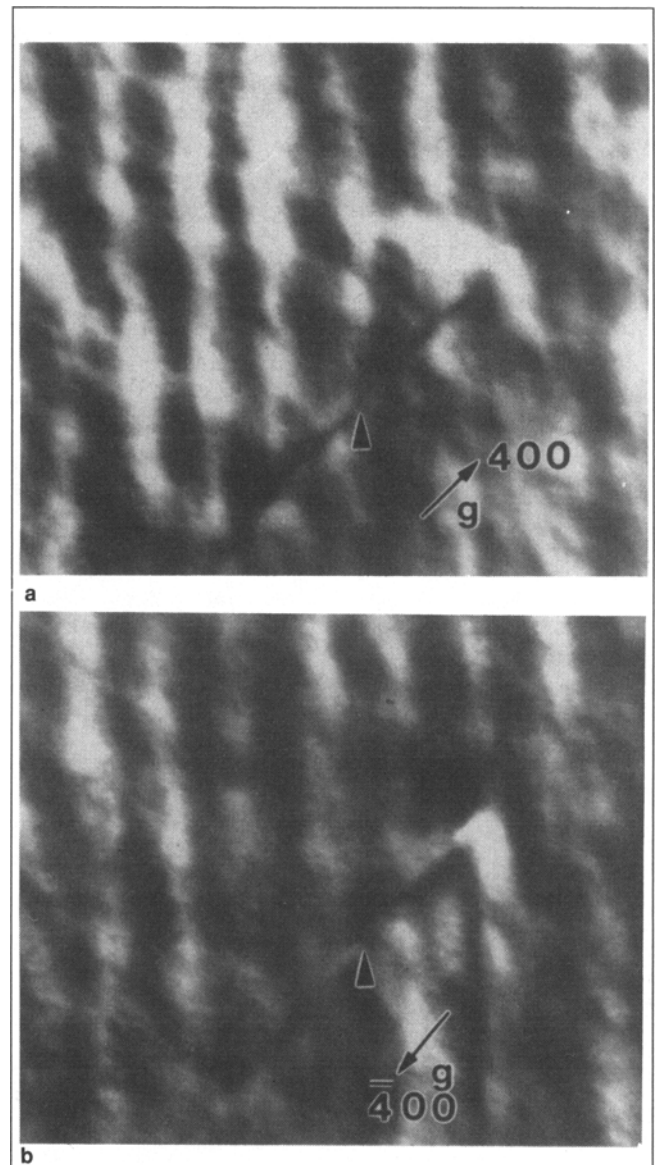


Fig. 4. Transmission electron microscopy (001) plan-view (a) (400) and (b) (400) dark field images of a $\text{Zn}_{1-x}\text{Mg}_x\text{S}_y\text{Se}_{1-y}$ film. The same Frank partial dislocation (marked by an arrowhead) is shown in both figures as reference. The contrast of surface buckling is reversed from (a) to (b).

[$\bar{1}01$] directions in a semi-periodic manner.

Composition Modulation Induced Surface Buckling of TEM Specimens

Figure 3 shows a (400) dark field image from a plan-view sample of the quaternary film after etching the GaAs substrate. In this figure, two kinds of contrast modulation along the [110] and [100] (but not [$1\bar{1}0$] or [010]) directions are observed. The period of the [110] modulation contrast is of ~40 to 50 nm. The contrast modulation along the [100] direction corresponds to striation-like contrast with modulation period of ~50 to 70 nm. When the sample is imaged using the [$\bar{2}20$] reflection, these striated structures exhibit speckle contrast while the [110] modulated strain contrast disappears. This observation is similar to the fine-

scale contrast reported in $In_{1-x}Ga_xAs_yP_{1-y}$ epitaxial layers.^{12,16,17} These striated structures are recognized as the contrast induced by the composition modulation seen in Fig. 1a and Fig. 3. It is important to note that no contrast modulation was observed along the [010] direction under [040] two-beam condition in TEM plan-view and cross-sectional images, while strong contrast modulation was observed along the [100] direction in the TEM cross-section images under [400] two-beam condition (see Fig. 1a). Thus, we believe that only one-dimensional composition modulation occurs in the $Zn_{1-x}Mg_xS_ySe_{1-y}$ films.

The contrast modulation along [110] became weaker under a [220] two-beam condition. Thus, this contrast does not correspond to composition-modulation contrast. Also, under (400) (Fig. 4a) and ($\bar{4}00$) (Fig. 4b) two-beam conditions, the contrast reversed sign with the change in the sign of g in dark field images, but did not reverse sign in bright field images. The contrast modulation along the [110] direction was also attenuated in thin areas, and under [400] weak-beam and [200] two-beam conditions. This kind of diffraction contrast effect has been studied in detail¹⁷ and is related to lattice plane bending near the surface of the TEM specimen due to stress relaxation. The contrast is induced by the relaxation of the shear stresses which accompany the quasi-periodic composition modulation. A consequence of specimen bending is the local change in the deviations from the Bragg condition that introduce an asymmetry in the dark-field images.¹⁷ Besides, a comparison of the intensities of the (400) and (200) two-beam conditions shows that the intensity of the dark-field images is significantly weaker under (200) than (400) two-beam conditions.¹⁷ In thin areas, however, the stresses are not high enough for buckling to occur.^{12,17} Thus, the stress relaxation of the TEM specimens induces the [110] modulated strain contrast.

This one-dimensional strain contrast is coupled with the one-dimensional [100] composition modulation contrast. In $In_xGa_{1-x}As_yP_{1-y}$ epitaxial layers,^{12,16,17} two-dimensional surface buckling along the [100] and [010] directions was associated with the two-dimensional composition modulation along these directions. It has been previously reported that the break up of the films into domains with different composition modulation directions causes periodic, localized bending of the planes at the film surface.¹² Thus, in our case, we believe that the development of the one-dimensional buckling in the $Zn_{1-x}Mg_xS_ySe_{1-y}$ film surface is a result of the strain relaxation in the thin specimen caused by the [100] one-dimensional composition modulation that develops at the growth surface.

Composition Modulation and Microtwins in Relaxed $Zn_{1-x}Mg_xS_ySe_{1-y}$ Layers

Figure 5a is a TEM (202) bright field image from a (010) cross-sectional $Zn_{1-x}Mg_xS_ySe_{1-y}$ /ZnSe buffer/GaAs heterostructure. The thickness of the ZnSe buffer layer is $\sim 270\text{\AA}$ and the total thickness of the quater-

nary film is $\sim 2.1\ \mu\text{m}$. Similar to Fig. 1a, composition modulation contrast is observed along the [100] direction in the $Zn_{1-x}Mg_xS_ySe_{1-y}$ film with a period of ~ 50 to $70\ \text{nm}$. Areas where RHEED studies were carried out are marked by arrowheads in Fig. 5. Microtwins (labeled T) are observed in the $Zn_{1-x}Mg_xS_ySe_{1-y}$ film; but contrary to Fig. 1a, no tweed contrast is observed in Fig. 5a even though the growth conditions for the quaternary layers were the same and only their thicknesses are different. TEM ($\bar{1}10$), (110), (100), and (010) diffraction patterns from the thicker films did not show streaky diffraction spots along the [001] growth direction which indicates that the lattice in the regions of different composition is relaxed and no local lattice distortion of a_1 exists. Thus, the lattice strain stored in the pseudomorphic quaternary films (see Fig. 1) relaxes when the thickness of the quaternary film is increased above critical thickness. Since no tetragonality of the lattice exists in the relaxed $Zn_{1-x}Mg_xS_ySe_{1-y}$ layers, no tweed contrast is observed (see Fig. 5).

Figure 5b is a TEM (004) dark field image from a (110) cross-sectional sample with total film thickness of $\sim 2.1\ \mu\text{m}$. No contrast for the composition modulation and no tweed-like strain contrast was observed. Again, this result indicates that there is no composition modulation along the [001] growth direction. Also, instead of the tweed contrast observed in Fig. 1

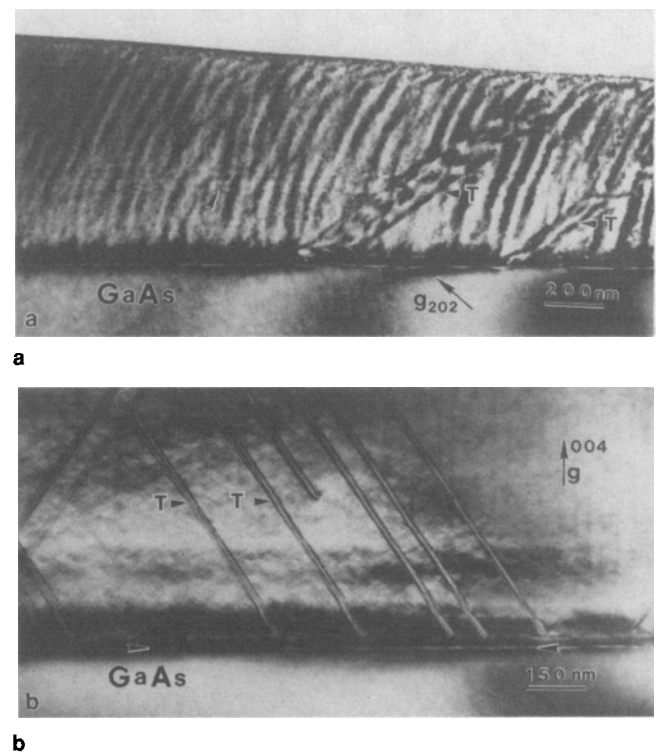


Fig. 5. (a) Transmission electron microscopy (010) cross section (202) and (b) TEM (110) cross section (004) bright field images of a $\sim 200\text{\AA}$ ZnSe cap layer/ $\sim 2.1\ \mu\text{m}$ $Zn_{0.76}Mg_{0.24}S_{0.33}Se_{0.67}$ /270Å ZnSe buffer/GaAs sample. Microtwins (labeled T) are observed in both (a) and (b), but composition modulation contrast is only observed in (a). The area with RHEED study is marked by an arrowhead in (a) and the ZnSe/GaAs interface is marked by arrowheads in (b).



Fig. 6. High resolution TEM (110) cross-sectional image from the ZnSe/GaAs interface of a sample with ~ 2 min Zn exposure on an As-stabilized GaAs substrate. A smooth 2–3 monolayer thick band with bright contrast along the ZnSe/GaAs interface is observed. The film was grown by the layer-by-layer growth mode from the initial stages of growth and no defects were observed.

for the quaternary layers with film thickness of ~ 0.72 μm (see Fig. 1), there are microtwins with a typical thickness of ~ 2 – 8 {111} planes that form to relax the misfit strain. These microtwins are probably formed by the successive nucleation and gliding of partial dislocations from the film surface to the interface on adjacent (111) planes as evidenced by RHEED. Most of the microtwins end at the $\text{Zn}_{1-x}\text{Mg}_x\text{S}_y\text{Se}_{1-y}/\text{ZnSe}$ interface as observed from the TEM (004) images obtained from (110), ($\bar{1}10$), (100), and (010) cross-sectional samples with total film thickness of ~ 2.1 μm .

Misfit Strain Induced Tweed-Twin Transformation

Our in-situ RHEED studies, showed that the surface of the film starts to become rough when the film thickness is ~ 0.8 – 1 μm . Our TEM (100)-type or (110)-type cross-sectional images, showed that the surface of the ZnSe cap layer is rough in the relaxed 2.1 μm thick film while it is flat for the pseudomorphic 0.72 μm thick film. The formation of microtwins probably contributes to the surface roughness of the relaxed $\text{Zn}_{1-x}\text{Mg}_x\text{S}_y\text{Se}_{1-y}$ film. Thus, as evidenced from the RHEED studies, the critical thickness for the break up of coherency in the $\text{Zn}_{1-x}\text{Mg}_x\text{S}_y\text{Se}_{1-y}/\text{ZnSe}$ buffer/GaAs heterostructure is ~ 0.8 – 1 μm for $0.24 \leq x \leq 0.28$ and $0.26 \leq y \leq 0.33$.

For epitaxial semiconductor heterostructures with low lattice mismatch, the generation of misfit dislocations is the usual mechanism for strain relaxation. Details on the strain relaxation mechanism via the dissociation of Frank partial dislocations have been proposed for N-doped ZnSe/GaAs.¹⁸ However, the formation of microtwins could also participate in the relaxation of the lattice mismatch.^{19,20} These defects for misfit accommodation are normally observed in systems with large lattice mismatch like SiC on Si. In our relaxed $\text{Zn}_{1-x}\text{Mg}_x\text{S}_y\text{Se}_{1-y}$ samples, we observed a density of microtwins of $\sim 1 \times 10^8/\text{cm}^2$ mostly in the $\text{Zn}_{1-x}\text{Mg}_x\text{S}_y\text{Se}_{1-y}$ layer and ending at the $\text{Zn}_{1-x}\text{Mg}_x\text{S}_y\text{Se}_{1-y}/\text{ZnSe}$ interface. From (110) and ($\bar{1}10$) cross-sectional images from this sample, we observed that these

microtwins are bounded by Shockley partial dislocations with a typical thickness of ~ 2 – 8 {111} planes as shown in Fig. 5b. The spacing between the microtwins on the $\text{Zn}_{1-x}\text{Mg}_x\text{S}_y\text{Se}_{1-y}/\text{ZnSe}$ interface varies in the range 0.05 to 0.1 μm . Also, from HRTEM images from this sample, a pure edge dislocation formed when two microtwins lying on two different {111} planes met at the $\text{Zn}_{1-x}\text{Mg}_x\text{S}_y\text{Se}_{1-y}/\text{ZnSe}$ interface. Both Shockley partials and pure edge-type dislocations have edge component on/or parallel to the film/substrate interface. Thus, the microtwins ending at the $\text{Zn}_{1-x}\text{Mg}_x\text{S}_y\text{Se}_{1-y}/\text{ZnSe}$ interface probably relax the misfit strain between these two layers. Furthermore, the x-ray spectra from this sample showed that the quaternary film is relaxed with a (004) peak at ~ 640 arc s from the GaAs peak and the value of FWHM from this peak is ~ 200 arc s. This result indicates that the quaternary film is relaxed with an average lattice constant $a_{\perp} = a_{\parallel} \sim 5.68 \text{ \AA}$ and the lattice mismatch between the $\text{Zn}_{1-x}\text{Mg}_x\text{S}_y\text{Se}_{1-y}$ film and the GaAs substrate is $\sim 0.46\%$. Assuming that the misfit strain between film and substrate is completely relaxed by microtwins bound by either $1/6\langle 112 \rangle$ -type Shockley partials or $1/2\langle 110 \rangle$ -type pure edge dislocations on the $\text{Zn}_{1-x}\text{Mg}_x\text{S}_y\text{Se}_{1-y}/\text{ZnSe}$ interface, the spacing between them should be ~ 0.05 to 0.09 μm in agreement with our results (see Fig. 5). Thus, we believe that the misfit strain between the $\text{Zn}_{1-x}\text{Mg}_x\text{S}_y\text{Se}_{1-y}$ and the ZnSe layers is relaxed by the generation of microtwins when the thickness of the $\text{Zn}_{1-x}\text{Mg}_x\text{S}_y\text{Se}_{1-y}$ films is > 0.8 – 1 μm .

As mentioned above, tweed structures in the pseudomorphic quaternary films with composition modulation are induced by the lattice misfit strain associated with the difference in covalent radii between Zn and Mg, and S and Se. Lattice tetragonality with local distortion should be maintained in order to produce tweed strain contrast. On the other hand, when the film is relaxed, there is no tetragonality and the tweed structures disappear as seen in Fig. 5. Thus, it is clear that there is a tweed-twin transformation induced by the relaxation of the lattice misfit strain during the growth of $\text{Zn}_{1-x}\text{Mg}_x\text{S}_y\text{Se}_{1-y}/\text{ZnSe}$ buffer/GaAs heterostructures.

Quality Control of the ZnSe/GaAs Interface

Another important consideration for the application of these materials which influences the performance of devices fabricated with them is the quality of the films. The lifetime of the light emitting diodes fabricated with these heterostructures depends greatly on the quality of the ZnSe-based/GaAs heterostructure. Defects, such as stacking faults and misfit dislocations can act as nonradiative recombination centers or sources for the formation of degradation defects in the active layers.¹⁰ The lifetime of a device is limited from a few hours to a few days. Thus, the density of stacking faults needs to be decreased to increase the lifetime of the device. In our case, only Frank partial dislocations originating at the interface between the 2D grown ZnSe buffer on As-terminated GaAs sub-

strates were observed. The density of Frank-type defects varied in the range from $5 \times 10^4/\text{cm}^2$ to $5 \times 10^7/\text{cm}^2$ for films grown under similar conditions. However, no misfit or Shockley partial dislocations were observed in any of the samples at either the Zn_{1-x}Mg_xS_ySe_{1-y}/ZnSe or ZnSe/GaAs interfaces. In contrast to the case of N-doped ZnSe/GaAs,¹⁸ no dissociation of the Frank-type partial dislocations to relax the lattice mismatch was observed in the composition modulated layers with film thicknesses of 0.72–2.1 μm . These results indicate that all the layers in the films were either pseudomorphic ($\sim 0.72 \mu\text{m}$) to the GaAs substrate or relaxed by microtwins (2.1 μm).

From the TEM dark field images, Frank-type partials were observed in areas with rough ZnSe/GaAs interface. These samples had a stacking fault density of $\sim 5 \times 10^7/\text{cm}^2$. It is important to note that these Frank-type partials form due to the roughness of the ZnSe/GaAs interface while the microtwins form to relax the strain in the quaternary layer and do not terminate at the ZnSe/GaAs interface but rather at the Zn_{1-x}Mg_xS_ySe_{1-y}/ZnSe interface. A recent study of the GaAs surface²¹ shows that an As-rich GaAs surface is inherently rough. A rough surface has a lower surface energy compared to a flat surface. Thermodynamically, an As-rich surface cannot exist as a complete As monolayer, but it can in a reconstructed surface in either the missing-dimer or multi-layer structure.²¹ Thus, an As-rich GaAs surface can give rise to films with rough interfaces. The surface roughness may trap point defects and contribute to a density of Frank partials of $\sim 5 \times 10^7/\text{cm}^2$.

On the other hand, a HRTEM image of a smooth ZnSe/GaAs interface is shown in Fig. 6 for a sample with ZnSe buffer layer grown on As-stabilized GaAs substrate. Prior to the growth of this film, the As-stabilized GaAs substrate surface was exposed to a Zn atmosphere for approximately 2 min. The Zn exposure produced a smooth and continuous bright band of ~ 2 – 3 interfacial layers along the coherent interface. Besides, the density of the Frank-type partials in this sample was less than $\sim 5 \times 10^4/\text{cm}^2$. No Shockley partial dislocations were observed in these samples probably because they were grown by 2D growth.²² In the present study, the films of highest quality were obtained when a flat surface was maintained by As stabilization of the GaAs surface followed by 2 min exposure to Zn to form a smooth ZnSe/GaAs interface.

CONCLUSIONS

We observed a one-dimensional composition modulation along the [100] direction which develops on the growing surface of the Zn_{1-x}Mg_xS_ySe_{1-y} films ($0.24 \leq x \leq 0.28$ and $0.26 \leq y \leq 0.33$) in both pseudomorphic and relaxed films. The composition modulation indicates that the solid solution of Zn_{1-x}Mg_xS_ySe_{1-y} films is not stable for these values of composition.²³ For pseudomorphic quaternary layers with film thickness below ~ 0.8 – $1 \mu\text{m}$, tweed strain contrast was observed in this layer originating at the Zn_{1-x}Mg_xS_ySe_{1-y}/ZnSe interface in addition to the composition modulation. The

origin of the tweed structure is explained by a localized distortion of the lattice along the growth direction, i.e., a variation in tetragonality for the domains with different composition. The larger tetrahedral radii of Mg and S compared to those of Zn and Se give rise to distortions of the lattice along the growth direction in regions of different composition in the Zn_{1-x}Mg_xS_ySe_{1-y} films. A schematic diagram of the modulated structure associated with the tweed strain contrast was suggested. On the other hand, the tweed strain contrast disappeared in relaxed Zn_{1-x}Mg_xS_ySe_{1-y}/ZnSe buffer/GaAs heterostructures with thickness above 1 μm . However, in these samples microtwins formed to relax the lattice misfit strain in the quaternary layers. These microtwins produce roughnesses of the film surface as evidenced by TEM and RHEED. In-situ RHEED studies suggested that the critical thickness for the lattice strain relaxation (tweed-twin transformation) in Zn_{1-x}Mg_xS_ySe_{1-y}/ZnSe buffer/GaAs heterostructure is ~ 0.8 – $1 \mu\text{m}$. Very high quality films were obtained by exposing the As-stabilized GaAs surface to Zn for ~ 2 min prior to the growth of the films. These films had no misfit dislocations or Shockley partial dislocations. They only contained Frank partial dislocations with a density lower than $5 \times 10^4/\text{cm}^2$.

ACKNOWLEDGMENTS

This work was supported by the 3M Company and the National Science Foundation contract No. DMR 9321957.

REFERENCES

1. M.A. Haase, J. Qiu, J.M. DePuydt and H. Cheng, *Appl. Phys. Lett.* 59, 1272 (1991).
2. H. Jeon, J. Ding, W. Patterson, A.V. Nurmikko, W. Xie, D.C. Grillo, M. Kobayashi and R.L. Gunshor, *Appl. Phys. Lett.* 59, 3619 (1991).
3. H. Okuyama, K. Nakano, T. Miyajima and K. Akimoto, *Jpn. J. Appl. Phys.* 30, L1620 (1991).
4. J.M. Gaines, R.R. Drenten, K.W. Haberern, T. Marshall, P. Mensz and J. Petruzzello, *Appl. Phys. Lett.* 62, 2462 (1993).
5. H. Okuyama, F. Hiei and K. Akimoto, *Jpn. J. Appl. Phys.* 31, L340 (1992).
6. Y. Morinaga, H. Okuyama and K. Akimoto, *Jpn. J. Appl. Phys.* 32, 678 (1993).
7. S. Itoh, N. Nakayama, T. Ohata, M. Ozawa, H. Okuyama, K. Nakano, A. Ishibashi, M. Ikeda and Y. Mori, *Jpn. J. Appl. Phys.* 32, L1530 (1993).
8. L. Pauling, *The Nature of the Chemical Bond* (New York: Cornell University Press, 1960), p. 246.
9. L.H. Kuo, L. Salamanca-Riba, B.J. Wu, J.M. DePuydt, S. Guha and G.M. Haugen, *Producibility of II-VI Materials and Devices*, Proc. SPIE Intl. Sym. on Optical Engineering and Photonics in Aerospace Sensing Conf., 2228, 134 (1994).
10. S. Guha, J.M. DePuydt, M.A. Haase, J. Qiu and H. Cheng, *Appl. Phys. Lett.* 63, 3107 (1993).
11. B.J. Wu, J.M. DePuydt, G.M. Haugen, G.E. Hofler, M.A. Haase, H. Cheng, S. Guha, J. Qiu, L.H. Kuo and L. Salamanca-Riba, submitted to *Appl. Phys. Lett.*
12. T.L. McDevitt, S. Mahajan and D.E. Laughlin, *Phys. Rev.* 45, 6614 (1992).
13. L. Salamanca-Young (Riba), S. Nahm, M. Wuttig, D.L. Partin and J. Heremans, *Phys. Rev.* B39, 10995 (1989).
14. S. K. Maksimov, *Microscopy of Semiconducting Materials*, ed. A.G. Cullis and N.J. Long, (London: Institute of Physics and Physical Society, 1991), p. 491.

15. I.M. Roberston and C.M. Wayman, *Phil. Mag. A* 48, 421, 443, 629 (1983).
16. S. Mahajan, B.V. Dutt, H. Temkin, R.J. Cava and W.A. Bonner, *J. Cryst. Growth* 68, 589 (1984).
17. M.M.J. Treacy, J.M. Gibson and A. Howie, *Phil. Mag. A* 51, 389 (1985).
18. L.H. Kuo, L. Salamanca-Riba, J.M. DePuydt, H. Cheng and J. Qiu, *Phil. Mag.* 69, 301 (1994).
19. W. Wegscheider, K. Eberl, H. Cerva and H. Oppolzer, *Appl. Phys. Lett.* 55, 448 (1989).
20. D.M. Hwang, S.A. Schwarz, T.S. Ravi, R. Bhat and C.Y. Chen, *Phys. Rev. Lett.* 66, 739 (1991).
21. T. Ohno, *Phys. Rev. Lett.* 70, 631 (1993).
22. L.H. Kuo, L. Salamanca-Riba, G. Hofler and B.J. Wu, *Phil. Mag.*, in press.
23. A.L. Roytburd and G. Sung, *Phase Transformations in Thin Films—Thermodynamics and Kinetics*, ed. M. Atzmon, A.L. Greer, J.M.E. Harper and M.R. Libera, (Pittsburgh, PA: Mater. Res. Soc., 1993), p.143.